

PROCEEDINGS OF SPIE

SPIDigitalLibrary.org/conference-proceedings-of-spie

Testbed for coupling starlight into fibers and astrophotonic instruments

Diab, Momen, Dinkelaker, Aline, Davenport, John, Madhav, Kalaga, Roth, Martin

Momen Diab, Aline N. Dinkelaker, John Davenport, Kalaga Madhav, Martin M. Roth, "Testbed for coupling starlight into fibers and astrophotonic instruments," Proc. SPIE 11451, Advances in Optical and Mechanical Technologies for Telescopes and Instrumentation IV, 114516G (13 December 2020); doi: 10.1117/12.2564720

SPIE.

Event: SPIE Astronomical Telescopes + Instrumentation, 2020, Online Only

Testbed for coupling starlight into fibers and astrophotonic instruments

Momen Diab^a, Aline N. Dinkelaker^a, John Davenport^a, Kalaga Madhav^a, and Martin M. Roth^a

^ainnoFSPEC, Leibniz Institute for Astrophysics Potsdam, An der Sternwarte 14482, Germany

ABSTRACT

We assembled a testbed to study coupling of starlight through atmospheric turbulence via astronomical telescopes into astrophotonic devices. The setup allows for varying the turbulence strength and investigating the effects of different levels of adaptive optics correction on the efficiency of integrated optics. In addition to recording optical powers and wavefront errors, focal plane images are captured from which spots sizes and Strehl ratios are also measured. Novel astrophotonic components proposed as alternatives to conventional optical instruments can therefore be qualified in terms of coupling efficiency and throughput on the testbed before they are tested on the sky.

Keywords: Astrophotonics, integrated optics, adaptive optics, atmospheric effects, starlight coupling

1. INTRODUCTION

Astrophotonic instruments offer an alternative to conventional free-space optics where setups behind astronomical telescopes can be kept at manageable sizes and weights and are therefore less costly and easier to environmentally control. Astrophotonic devices manipulate, i.e. split, filter, disperse, and interfere, starlight via structures of contrasting refractive indices inside waveguides contrary to bulk optics that reflect or refract light at air/glass interfaces.^{1,2} This integrated approach reduces the size manifold and cuts reflection losses common to optical trains. Some astrophotonic technologies like planar beam combiners,³ discrete beam combiners (DBC)s⁴ and fiber Bragg grating (FBG) OH suppression filters⁵ will only function as intended if their waveguides sustain a single, fundamental mode. Others like arrayed waveguide gratings (AWGs)⁶ will have their performance impaired as the number of modes at their intake waveguides increases. The most pressing challenge to photonic devices is efficient coupling into them from free space. For ground-based telescopes, starlight arrives at the entrance pupil with a distorted wavefront due to Earth's atmosphere. This translates into a speckle intensity pattern at the focal plane that poorly couples into the commonly Gaussian fundamental mode of single-mode waveguides. Adaptive optics (AO) can help improve coupling by correcting the incident wavefront to produce a point spread function (PSF) that is more favorable to waveguides but the quality of correction, i.e. the residual error in the resulting wavefront, depends on the number of actuators, the bandwidth of the control loop, and the brightness of the guide star among other factors. Therefore this correction, in most practical scenarios, is only partial and the theoretical maximum coupling into the single-mode regime cannot be achieved.

Increasing the number of modes at the input waveguide can boost the coupling efficiency even if only a low-order adaptive optics (LOAO) system of ~ 100 degrees of freedom is employed. This presents a bargain to certain types of astrophotonic devices that can still operate on an input beam of few modes without compromising performance greatly. Alternatively, the few-mode beam in the input waveguide can be converted using a photonic lantern into a number of single-mode beams, where if the numbers of modes and single-mode fibers (SMFs) are matched, the conversion is lossless.⁷ A multiplexed astrophotonic instrument that has multiple replicas of the same photonic device can then be fed by the SMFs to recover most, if not all, of the flux collected by the telescope.^{8,9}

The Astrophotonics Group at the Leibniz Institute for Astrophysics Potsdam (AIP),¹⁰ among others, is developing a number of near-IR astrophotonic technologies, e.g. AWGs,¹¹ photonic echelle gratings,¹² FBG

Further author information: (Send correspondence to M.D.)

M.D.: E-mail: mdiab@aip.de

OH suppression filters,¹³ DBCs,¹⁴ and photonic reformatters,¹⁵ that have the potential of replacing their bulk optics counterparts once their readiness level is sufficient. Many astronomy applications are, however, photon-starved and losses must be kept at minimum if a new concept is to be adopted. The bottleneck in the photons budget of an astrophotonic device is the coupling loss at the telescope focal plane. To study coupling under varying circumstances of turbulence strength, AO correction levels, misalignments, focal ratios, wavelength, and waveguide modes, we built a testbed around an LOAO setup where one can quantify the coupling efficiency and its dynamics with emulated atmospheric turbulence in the lab. In this proceeding, we describe the main aspects of the setup and comment on some of the obtained results.

Sec. 2 describes the main components of the setup and their function while Sec. 3 provides details about some of the features of the controlling software. In Sec. 4, examples of some results that one can obtain are given with a discussion about the testbed capabilities and limitations.

2. TESTBED HARDWARE

The testbed is illustrated in Fig. 1. At its core is an ALPAO LOAO system that corrects wavefronts distorted by an atmosphere emulator upstream. Two laser sources are used, one in the visible to simulate a guide star and one in the near-IR to simulate a science target. A pigtailed DFB laser diode with a center wavelength $\lambda = 1550$ nm and an FWHM linewidth $\Delta f = 1$ MHz simulates the science target. Wavelength tunability over a small range, $\Delta\lambda = 8$ nm, is possible with a temperature controller allowing (limited) spectral response measurements. A Fabry-Pérot single-mode laser diode with a central wavelength $\lambda = 775$ nm and maximum FWHM linewidth $\Delta\lambda = 2$ nm is used to simulate the guide star. Both beams, launched from SMFs, are collimated and then expanded to 24 mm diameters using achromats and Galilean telescopes, respectively. A beam splitter is used to overlap the two beams before a phase distortion is introduced in the wavefronts.

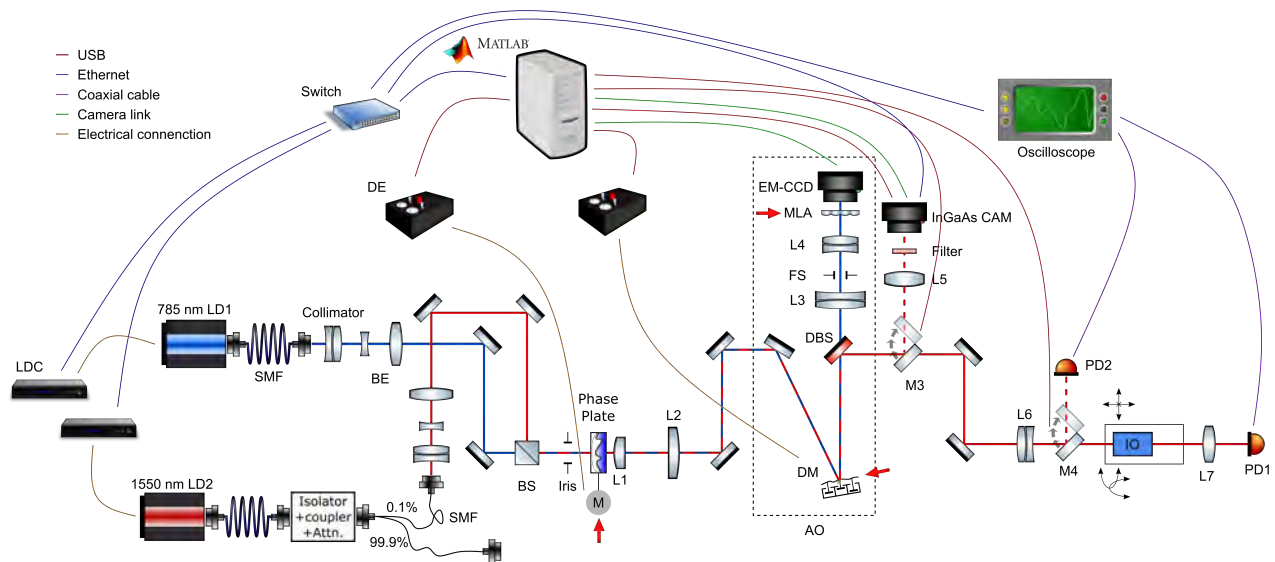


Figure 1. Schematic of the testbed. LDC: laser diode controller, DE: drive electronics, SMF: single-mode fiber, LD: laser diode, BE: beam expander, BS: beam splitter, M: stepper motor, DM: deformable mirror, DBC: dichroic, FS: field stop, PD: photodiode, IO: integrated optic. Red arrows indicate conjugated pupil planes. The fiber coupler for the 1550 nm LD provides a high power beam that can be launched from either end to ease alignment.

The combined beams are passed through a phase screen that emulates an atmospheric turbulence layer. The phase screen from LEXITEK¹⁶ is a sandwich of 4 optical disks. The outer 2 are B-K7, AR-coated protective windows while the inner 2 are polymers of nearly matched refractive indices ($\Delta n < 0.001$). A pattern that has Kolmogorov statistics with Fried parameter $r_0 = 0.6$ mm is impressed on the two polymers before they are bonded. Turbulence strength D/r_0 can be controlled by clipping the emerging beam by an iris down to the

required size. The plate is mounted on a rotary stage that can rotate at a maximum of 100 rpm to allow for measurements at different realizations from the screen and simulate wind velocities. For the smaller beams, a translation stage moves the plate laterally to make use of most of the screen area. An afocal system (L1 - L2) is then needed to image the phase screen with the correct magnification on the deformable mirror (DM) of the AO system. Folding mirrors on kinematic mounts allow for independently realigning the beam to the optical axis every time the afocal system is replaced to vary the turbulence strength. A removable cage system facilitates the replacement of the lenses.

The AO system has a Shack-Hartmann wavefront sensor (WFS) with a 16×16 subapertures microlens array (MLA) in front of an EM-CCD that has a quantum efficiency $> 75\%$ in the visible and a full frame rate of 1 kHz. The DM from ALPAO has a continuous face sheet membrane controlled by 97 magnetic voice coils arranged in an octagonal configuration that can achieve a tip/tilt (P-V) stroke of $60 \mu\text{m}$ and an inter-actuator stroke $> 3 \mu\text{m}$ at a response time $< 1 \text{ ms}$. In a closed loop configuration, the distorted beam is first reflected off of the DM toward a dichroic mirror that passes the visible beam through to a beam reducer (L3 - L4) that resizes the beam to match the pupil at the MLA. The MLA is placed at the DM conjugate plane with the EM-CCD detector at the focal plane of the MLA, 7 mm away. The AO setup is aligned by the vendor and no realignment is necessary upon varying the turbulence strength. The DM however must be at the exit pupil, i.e. the conjugate plane of the phase screen, and the afocal system (L1 - L2) is placed appropriately depending on the magnification with the exact distances obtained from ZEMAX calculations (see Fig. 2).

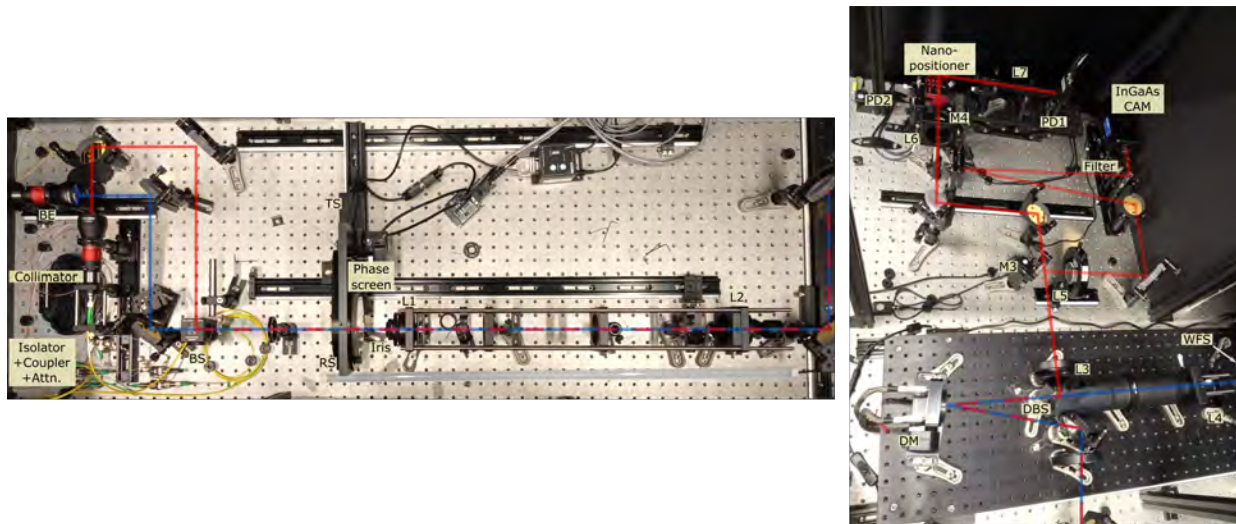


Figure 2. Picture of the testbed. Left: sources and atmospheric emulation setup. RS: rotary stage. TS: translation stage. Right: adaptive optics, coupling and imaging setups.

The corrected science beam reflected out of the AO system can be directed toward a focusing lens where the PSF is imaged with a C-RED2 InGaAs camera. The focusing lens (L5) has a long focal length $f = 1 \text{ m}$ to enlarge the PSF on the detector and thus increase the resolution. With the diameter of the DM, $\phi = 13.5 \text{ mm}$, the Airy disk of the diffraction-limited PSF has a linear size of 0.28 mm at $\lambda = 1550 \text{ nm}$. This is sampled by $\sim 19 \times 19$ pixels on the detector, guaranteeing that larger speckle patterns are well sampled for any further post-processing. The corrected beam can also be passed to a coupling lens with a 6-axis positioner at the focal plane. Fibers and integrated optics components can be precisely aligned to the optical axis at the focus with a LUMINOS nano-positioner. A 10 nm resolution can be achieved for x and y alignment while 50 nm is possible for the less stringent z axis. Pitch and yaw can be adjusted with a resolution of 0.2 arcsec . The spot at the output of the component under test is imaged by a coated convex lens (L6) onto a photodiode (PD). This arrangement allows for measuring the total output power of the diverging beam out of the waveguide without the need to arbitrarily placing the PD close to the component. By choosing the right lens, the imaged spot can be made small enough to fit inside the active area of the PD within the limits allowed by conservation of étendue.

To measure the total power available for coupling at the aperture, a flip mirror (M4) reflects the converging beam behind L6 toward a second PD aligned at the focus. Coupling efficiency can thus be quantified. Flip mirrors instead of beam splitters are used to avoid non-common path aberrations (NCPA) and the chromatic response of BSs in regard to split ratios. A 200 MHz, 8 bits oscilloscope is used to average and digitize the voltages of the PDs.

All components are centrally controlled by an Intel i5-8500, 3.0 GHz, 6 cores processor and 16 GB RAM running a Matlab script. The pure delay between the end of a WFS exposure and generating the DM commands (as measured by ALPAO) is about 1.38 ms. Taking the frame rate of the WFS and the DM response time into account, the maximum Greenwood frequency that can be tracked is ~ 20 Hz.

Realignment of tip/tilt and defocus are usually required before a measurements run. The DM mount is adjusted to reduce tip/tilt to lower than $0.1 \mu\text{m}$ rms and the afocal system (L1 - L2) is adjusted to correct defocus. A calibration is then performed to record the influence functions and calculate the eigenvalues of the influence matrix. A realignment is required anytime the largest and the smallest eigenvalues differ by more than an order of magnitude.

3. CONTROL SOFTWARE

Closing the loop and driving the DM is done using ALPAO Core Engine (ACE).¹⁷ ACE is a Matlab environment, object-oriented toolbox that provides classes for interfacing the DM and the WFS and allows different modes of operation, e.g. closed loop, feed forward with Zernikes, zonal and modal reconstruction. Data acquisition and control of the rest of the equipment, i.e. LDs, phase screen, InGaAs camera, flip mirrors, translation stage, and oscilloscope, are also done with Matlab.

We wrote Matlab scripts to automate measurements of coupling efficiencies, capture PSF images and collect relevant wavefront information. Due to the stochastic nature of atmospheric turbulence, one is usually interested in metrics averaged over an ensemble of phase screens for variables sensitive to atmospheric effects, e.g. number of speckles in the PSF, wavefront error or coupling efficiency of light into a waveguide. The script therefore rotates the phase screen in steps and records the measurements from the 2 PDs and the 2 cameras, consequently.

Objects from ACE classes are used to control the AO system as desired. The effects of closing the loop, compensating for tip/tilt only or correcting with a limited number of modes on coupling and the anatomy of the PSF can all be tested seamlessly. Post-processing of PSF images yields additional information about the Strehl ratio (SR), encircled energy (EE) and the centroid shift, i.e. image motion. Wavefront measurements are also recorded.

The LDs currents are adapted by the software to maximize the PDs utilization, i.e. make full use of its dynamic range. The integration time of the InGaAs camera is then automatically set to prevent saturation while maintaining the highest possible SNR. Moreover, the software performs the necessary dark current and background subtractions for the PDs and the InGaAs camera.

Besides analyzing the PSF, the InGaAs camera can also be used to provide feedback for correcting the residual tip/tilt errors in the IR beam induced by temperature variations after alignment. Temperature and humidity at the DM, the nano-positioner, and the MLA are monitored in case creep and memory effects in the DM¹⁸ are suspected of causing any anomalies seen in long-term open loop experiments.

4. DISCUSSION ON THE TESTBED LIMITATIONS

To give an impression of the capabilities of the testbed, we present here examples of the results one can obtain for a turbulence strength of $D/r_0 = 8.3$ and the FG025LJA multimode fiber from THORLABS. Fig. 3 shows an example of the data collected for one measurement point. The trends in Fig. 4 show the variations in coupling efficiency and wavefront rms errors across the phase screen.

The PDs are the highly sensitive PDF10C from THORLABS. With a noise equivalent power of $NEP = 7.5 \text{ fW}$, they can measure coupling efficiencies as small as 75×10^{-6} . The two PDs are calibrated against each other over their dynamic range and the calibration table is made available for the coupling calculations script. Optical

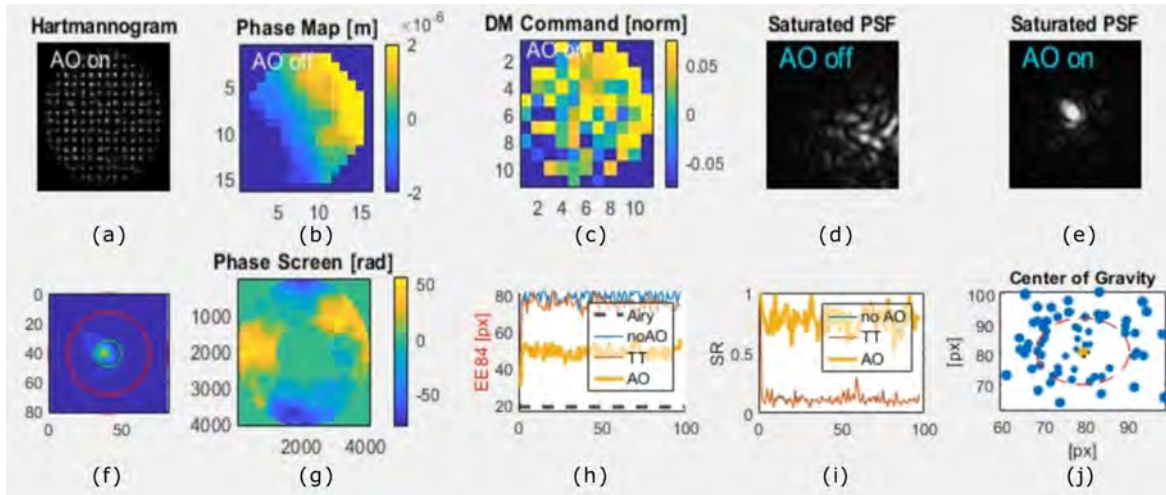


Figure 3. Cameras images and calculated parameters for one instance. (a) and (b) WFS image and the calculated phase, respectively. (c) commands sent to the DM by ACE. (d) and (e) PSFs before and after correction, respectively. (f) PSF containment within fiber core. (g) phase screen. (h) 84% encircled energy. (i) Strehl ratio. (j) scatter plot of PSFs centroids distribution around the fiber before tip/tilt correction.

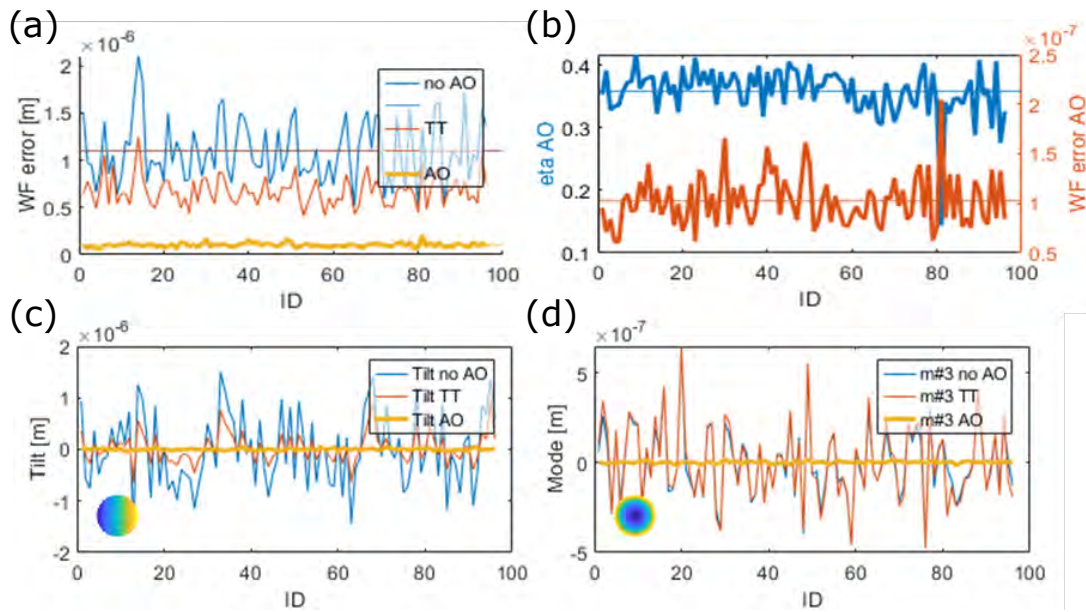


Figure 4. Coupling efficiency for a circular, step-index 6 modes fiber and wavefront errors across the phase screen. (a) rms wavefront error for the uncorrected case (blue), tip/tilt compensated (orange), and AO corrected case (yellow). (b) coupling efficiency and rms wavefront error for the AO corrected case. (c) and (d) variations of tilt and defocus across the screen, respectively.

power measurements taken for one instance of a phase screen, are averaged for a few seconds in the oscilloscope to minimize the effect of electronic noise in the PDs.

For cases of high turbulence strength ($D/r_0 > 15$), the loop might diverge due to the highest order modes having too small eigenvalues, i.e. the influence matrix being ill-conditioned, or the wavefront error being greater than the maximum DM stroke. The software optimizes the number of modes accordingly by filtering as many higher order modes as necessary to prevent the loop from diverging.

The largest unobstructed beam diameter that can be passed through the atmosphere emulator is 24 mm limiting the turbulence strength to $D/r_0 = 40$. The complete aperture of the screen with a diameter of 83 mm can, in theory, be used but with an obscuration of $\sim 40\%$. For small beams, the limiting factor is the magnification (L2/L1) that one requires to enlarge the beam to match the aperture of the DM.

The testbed components are optimized for the whole H-band but a tunable or a broadband NIR light source is required to perform spectral measurements. For temporal response measurements, the phase screen can be spun continuously by the rotary stage but the limitation of the control loop bandwidth is set by the 6 cores, 3 GHz PC used to close the loop. Astronomy grade AO systems in contrast have real time computers with pure delays in the order of $\sim 100 \mu\text{s}$.

5. CONCLUSIONS AND OUTLOOK

Upcoming innovative photonic technologies, although outperforming in many aspects, need to couple and transmit light as well as their bulk optics analogs before they are considered for facility instruments in photon-starved applications. We presented a testbed for starlight coupling that we plan to use to quantify coupling losses due to atmospheric turbulence, diffraction effects, and misalignments for a number of astrophotonic components. The gain that AO can provide to coupling light into few-mode and single-mode waveguides can also be studied under variant forms of correction owing to the flexibility of ALPAO's AO system. The software of the testbed collects data on power measurements, PSF images, and wavefront errors for an ensemble of phase screens. The user therefore attains comprehensive knowledge about the limitations of their integrated optic in terms of coupling and throughput. The computer used currently to control the AO loop reduces the Greenwood frequency of the system and limits the usefulness of temporal measurements for predicting on-sky performance of proposed components. A real time controller along with tunable broadband sources will increase the temporal and spectral capabilities of the testbed.

ACKNOWLEDGMENTS

The authors acknowledge financial support from the Federal Ministry of Education and Research (BMBF) under grant number 03Z22AN11.

REFERENCES

- [1] Bland-Hawthorn, J. and Leon-Saval, S. G., "Astrophotonics: molding the flow of light in astronomical instruments [Invited]," *Optics Express* **25**, 15549–15557 (June 2017). Publisher: Optical Society of America.
- [2] Minardi, S., Harris, R., and Labadie, L., "Astrophotonics: astronomy and modern optics," *arXiv:2003.12485 [astro-ph]* (Mar. 2020). arXiv: 2003.12485.
- [3] Eisenhauer, F., Perrin, G., Brandner, W., Straubmeier, C., Richichi, A., Gillessen, S., Berger, J. P., Hippler, S., Eckart, A., Schöller, M., Rabien, S., Cassaing, F., Lenzen, R., Thiel, M., Clénet, Y., Ramos, J. R., Kellner, S., Fédou, P., Baumeister, H., Hofmann, R., Gendron, E., Boehm, A., Bartko, H., Haubois, X., Klein, R., Dodds-Eden, K., Houairi, K., Hormuth, F., Gräter, A., Jocou, L., Naranjo, V., Genzel, R., Kervella, P., Henning, T., Hamaus, N., Lacour, S., Neumann, U., Haug, M., Malbet, F., Laun, W., Kolmeder, J., Paumard, T., Rohloff, R.-R., Pfuhl, O., Perraut, K., Ziegleder, J., Rouan, D., and Rousset, G., "GRAVITY: getting to the event horizon of Sgr A*," in [*Optical and Infrared Interferometry*], **7013**, 70132A, International Society for Optics and Photonics (July 2008).
- [4] Minardi, S., "Nonlocality of coupling and the retrieval of field correlations with arrays of waveguides," *Physical Review A* **92**, 013804 (July 2015).
- [5] Bland-Hawthorn, J., Ellis, S. C., Leon-Saval, S. G., Haynes, R., Roth, M. M., Löhmannsröben, H.-G., Horton, A. J., Cuby, J.-G., Birks, T. A., Lawrence, J. S., Gillingham, P., Ryder, S. D., and Trinh, C., "A complex multi-notch astronomical filter to suppress the bright infrared sky," *Nature Communications* **2**, 581 (Dec. 2011). Number: 1 Publisher: Nature Publishing Group.
- [6] Bland-Hawthorn, J. and Horton, A., "Instruments without optics: an integrated photonic spectrograph," in [*Ground-based and Airborne Instrumentation for Astronomy*], **6269**, 62690N, International Society for Optics and Photonics (2006).

- [7] Leon-Saval, S. G., Birks, T. A., Bland-Hawthorn, J., and Englund, M., “Multimode fiber devices with single-mode performance,” *Optics Letters* **30**, 2545 (Oct. 2005).
- [8] Bland-Hawthorn, J., Lawrence, J., Robertson, G., Campbell, S., Pope, B., Betters, C., Leon-Saval, S., Birks, T., Haynes, R., Cvetojevic, N., and Jovanovic, N., “PIMMS: photonic integrated multimode microspectrograph,” in [*Ground-based and Airborne Instrumentation for Astronomy III*], **7735**, 77350N, International Society for Optics and Photonics (July 2010).
- [9] Diab, M., Dinkelaker, A. N., Davenport, J., Madhav, K., and Roth, M. M., “Starlight coupling through atmospheric turbulence into few-mode fibers and photonic lanterns in the presence of partial adaptive optics correction,” *arXiv:2011.13423 [astro-ph, physics:physics]* (Nov. 2020). arXiv: 2011.13423.
- [10] Roth, M. M., Löhmansröben, H.-G., Kelz, A., and Kumke, M., “innoFSPEC: fiber optical spectroscopy and sensing,” in [*Advanced Optical and Mechanical Technologies in Telescopes and Instrumentation*], **7018**, 70184X, International Society for Optics and Photonics (July 2008).
- [11] Stoll, A., Zhang, Z., Haynes, R., and Roth, M., “High-Resolution Arrayed-Waveguide-Gratings in Astronomy: Design and Fabrication Challenges,” *Photonics* **4**, 30 (June 2017). Number: 2 Publisher: Multidisciplinary Digital Publishing Institute.
- [12] Stoll, A., Wang, Y., Madhav, K., and Roth, M., “Integrated échelle gratings for astrophotonics,” in [*Advances in Optical Astronomical Instrumentation 2019*], **11203**, 112030Z, International Society for Optics and Photonics (Jan. 2020).
- [13] Rahman, A., Madhav, K., and Roth, M. M., “Complex phase masks for OH suppression filters in astronomy: part I: design,” *Optics Express* **28**, 27797–27807 (Sept. 2020). Publisher: Optical Society of America.
- [14] Nayak, A. S., Poletti, T., Sharma, T. K., Madhav, K., Pedretti, E., Pedretti, E., Labadie, L., and Roth, M. M., “Chromatic response of a four-telescope integrated-optics discrete beam combiner at the astronomical L band,” *Optics Express* **28**, 34346–34361 (Nov. 2020). Publisher: Optical Society of America.
- [15] Pedretti, E., Harris, R. J., Minardi, S., Tepper, J., Davenport, J., Hottinger, P., Anagnos, T., Shankar Nayak, A., Quirrenbach, A., Labadie, L., Haynes, R., Haynes, D. M., Herrero Alonso, Y., and Deka, P. J., “NAIR: novel astronomical instrumentation through photonic reformatting,” in [*Advances in Optical and Mechanical Technologies for Telescopes and Instrumentation III*], Geyl, R. and Navarro, R., eds., 20, SPIE, Austin, United States (July 2018).
- [16] Ebstein, S. M., “Nearly index-matched optics for aspherical, diffractive, and achromatic-phase diffractive elements,” *Optics Letters* **21**, 1454–1456 (Sept. 1996). Publisher: Optical Society of America.
- [17] Schimpf, A., Micallef, M., and Charton, J., “1500Hz adaptive optics system using commercially available components,” in [*Adaptive Optics Systems IV*], **9148**, 914851, International Society for Optics and Photonics (July 2014).
- [18] Bitenc, U., Bharmal, N. A., Morris, T. J., and Myers, R. M., “Assessing the stability of an ALPAO deformable mirror for feed-forward operation,” *Opt. Express, OE* **22**, 12438–12451 (May 2014). Publisher: Optical Society of America.